Preparation and tribological properties of $Ti_3C_2T_x$/TiO_2 composite material

Z. P. Hou, H. Li, X. H. Zhang[*]
*School of Mechanical Engineering, Jiangsu University of Technology,
Changzhou 213001, Jiangsu Province, China*

$Ti_3C_2T_x$/TiO_2 composite materials were successfully prepared by hydrothermal reaction method. The phase structure and morphology of the samples were analyzed by X-ray diffractometer and scanning electron microscope. The results show that TiO_2 particles are evenly distributed between the layers and on the surface of $Ti_3C_2T_x$ nanosheets. The prepared composite materials were added to PAO6 base oil, and the MDW-02 friction and wear testing machine was used to study the effects of material addition concentration, working load and working speed on the tribological properties of lubricating oil. The friction test results show that the introduction of $Ti_3C_2T_x$/TiO_2 composite material can reduce friction, and the maximum reduction of friction and wear was achieved under additive concentration of 1.0 wt%. By scanning electron microscopy analysis of the wear scars, it was confirmed that the prepared nanocomposites repaired the scratched surface and formed a uniform lubricating film, which helped to improve the tribological properties of the base oil.

1. Introduction

Friction and wear are ubiquitous phenomena in daily life, and they are the main causes of energy loss and mechanical failure. According to statistics, about 80% of mechanical failures in the world are caused by parts wear, and 30% of energy consumption comes from friction[1]. Therefore, taking effective measures to reduce friction and wear between mechanical parts has become an urgent issue for researchers. Through continuous exploration and research, scholars have discovered that rational use of lubricants is one of the best methods[2]. In order to improve the lubrication performance, appropriate additives are generally added to lubricating oil[3]. In recent years, the application and exploration of nanomaterials in tribology have attracted more and more attention due to their unique properties in lubrication and tribology, such as anti-wear, friction reduction, and high load-bearing capacity[4].

MXene is a new type of nanomaterial, which is generally prepared by selective etchings of the MAX phase, which is a layered hexagonal crystal system (space group $P6_3$/mmc), with tightly packed M layers interlaced with pure A atomic layers, and X atoms filling the octahedral void of M[5]. The M-A bond in the MAX phase is a weaker ionic bond[6], and the A atomic layer has higher

reactivity. The M-X bond is mainly a strong covalent bond and is very stable. Therefore, the A-layer atoms can be selectively etched through appropriate methods to obtain MXene materials[7].

The general formula of the MXene structure is $M_{n+1}X_nT_x$, where M represents an early transition metal element[8], X represents the carbon or nitrogen element, and T_x indicating the functional groups (-O, -OH, -Cl, or -F, etc.) that are attached to the surface of MXene during the etching process[9]. Common ones include Ti_3C_2, Ti_2C, Ta_4C_3, $(Ti_{0.5}, Nb_{0.5})_2C$, $(V_{0.5}, Cr_{0.5})_3C_2$, etc[10-13]. During the exploration of MXene material properties, researchers found that MXene has a layered structure and properties similar to graphene, molybdenum disulfide, etc., such as high electronic conductivity, more surface-active sites, and excellent mechanical flexibility[14]. Moreover, the van der Waals force between the layered structures is weak and easy to peel off, giving it good lubrication properties. At present, MXene is widely used in research fields such as electrochemistry, energy storage, and sensors, and its application in the field of tribology has also received attention. For example, Liu et al.[15] explored the effects of $Ti_3C_2T_x$ concentration and exfoliation degree on the tribological properties of $Ti_3C_2T_x$ nanosheets as PAO8 base oil additives.

As a stable transition metal oxide, TiO_2 has excellent photocatalytic performance in the decomposition of organic pollutants, and also shows good corrosion resistance and antibacterial performance in the fields of corrosion prevention and biomedicine[16-20]. In recent years, the application of TiO_2 in the field of friction has also attracted much attention. Mirjavadi et al. [21] conducted a tribological analysis of TiO_2 nanoparticles as additives. Song [22] reported that TiO_2 nanoparticles modified with trifluoracetic acid as additives improved the friction-reduction and anti-wear abilities of the phenolic coating. In the process of continuous exploration, it was discovered that TiO_2 can form a good titanium film during friction and exhibit good lubrication properties, making it a promising lubrication additive [23,24]. Furthermore, recent studies have shown that composite nanomaterials exhibit better tribological properties than single-component nanomaterials [25-27]. Studies have shown that $Ti_3C_2T_x$ nanomaterials and TiO_2 nanoparticles as additives are good at anti-wear and anti-friction, respectively. Therefore, $Ti_3C_2T_x/TiO_2$ nanocomposites promise having both well anti-wear and anti-friction tribology properties.

In this work, $Ti_3C_2T_x/TiO_2$ composite nanomaterials were prepared a hydrothermal method. The structure and morphology of the prepared nanomaterials were characterized by XRD and SEM. The tribological behavior of the prepared nanomaterials in PAO6 base oil was studied by a MDW-02 reciprocating friction and wear testing machine. The wear scars on the surface of the steel disc were observed, and the friction reduction and wear resistance mechanism of nanomaterials as lubricating oil additives was proposed.

2. Experimental

2.1. Preparation of $Ti_3C_2T_x$ and TiO_2 nanoparticles

$Ti_3C_2T_x$ was prepared by chemical etching Ti_3AlC_2[28]. In a typical method, 2 g Ti_3AlC_2 was slowly added into 40 mL hydrofluoric acid solution under 200 rpm magnetic stirring at 25 ℃ for 24 h. The suspension was subsequently centrifuged at 3500 rpm for 5 min to remove the soluble fluorides. The solution was then centrifuged and rinsed several times with deionized water until the pH of the solution reached 5-6. The final precipitate was collected and dried in a vacuum oven at 80 °C for 24 h.

TiO$_2$ nanoparticles were synthesized by a hydrothermal method. Firstly, 1.6 mL tetrabutyl titanate was added to the mixed solution of distilled water (1ml) and acetic acid (50ml), continue stirring for 30min. Then the resulting white suspension was transferred into a 50ml Teflon-lined stainless-steel autoclave and sealed tightly, heated at 150°C for 12 h and then naturally cooled down to room temperature. The white precipitates were collected by centrifugation and washed with distilled water and absolute ethanol for several times, and finally dried in vacuum at 60°C for 24 h.

2.2. Preparation of Ti$_3$C$_2$T$_x$/TiO$_2$

First, 0.6g Ti$_3$C$_2$T$_x$ was dispersed into 30 ml of deionized water and ultrasonicated for 30 minutes. Then, 1.7 mL of tetrabutyl titanate was added to 9 mL of absolute ethanol, stirred for 10 min, and then slowly added to the Ti$_3$C$_2$T$_x$ solution. Stir the mixed solution for 3 hours until the mixed solution turns gray and has no precipitation, and then transfers it to a Teflon-lined autoclave and maintained at 150 °C for 12 h. By natural cooling down to room temperature, the resulting sample was washed three times alternately using deionized water and alcohol, dried in an oven at 60 °C for 24 h to obtain the final product.

2.3. Material characterization

The X-ray diffraction (XRD) patterns were recorded by a Bruker XPert PRO MPDX X-ray powder diffractometer with Cu Ka radiation (λ = 0.1546 nm). The 2θ range used in the measurement was from 10° to 80° and the scanning rate was 5°min^{-1} and the test voltage was 40KV, the current was 30mA. The microstructure and morphology of the prepared samples were investigated by scanning electron microscopy (FE-SEM, QUAN-TA FEG250).

2.4. Tribological performance test

The prepared materials were added to PAO6 base oil with different mass percentages to prepare lubricating oil. The MDW-02 reciprocating friction and wear testing machine was used to test the tribological properties of the lubricating oil in the ball-disk friction method. The steel plate material used in the test is 45# steel. Before the test, the surface was polished with 1200# sandpaper to make the surface roughness Ra value approximately 0.18~0.20μm, and ultrasonically cleaned with alcohol. The diameter of the steel ball used for testing is 3 mm, the material is GCr15, and the hardness is HRC60-65. The working load is 5~20N, the working speed is 120~300rpm, the working time is 10min, and the reciprocating stroke is 10mm.

3. Results and discussion

3.1. Material structure and morphology analysis

Fig.1 shows the XRD pattern of Ti$_3$AlC$_2$, Ti$_3$C$_2$Tx, TiO$_2$, and TiO$_2$/Ti$_3$C$_2$T$_x$ composite material. Fig. 1a is the XRD pattern of MAX phase powder (Ti$_3$AlC$_2$) and Ti$_3$C$_2$T$_x$ MXene. By comparison, the XRD pattern presented is consistent with the results in the literature 15, and the characteristic peaks of Ti$_3$C$_2$ (002), (004), (006), (105) and (110) crystal faces appear at 2θ=8°, 18°, 28°, 42° and 62°, respectively. The characteristic peaks (002) and (004) of MAX phase powder (Ti$_3$AlC$_2$) are 9.7° and 19.4°, respectively, while the positions of the characteristic peaks

corresponding to Ti_3C_2 MXene are 9.1° and 18.4°. In addition, the characteristic peaks (104) of the MAX phase powder (Ti_3AlC_2) at 39.2° disappear, and the characteristic peaks at $2\theta=8°$, 34°, 38°, and 42° show very weak and wider peaks in the diffraction of Ti_3C_2. These changes indicate that the aluminum layer has been successfully removed, and the crystal face spacing of Ti_3C_2 MXene corresponding to the crystal direction has increased[29].

Fig. 1b presents the XRD pattern of the as-prepared TiO_2, which is consistent with the standard TiO_2 PDF card (PDF#21-1272). Fig. 1c shows the XRD patterns of Ti_3C_2, TiO_2 and Ti_3C_2/TiO_2 nanocomposites from bottom to top. According to the XRD pattern of Ti_3C_2/TiO_2 nanocomposite, all the diffraction peaks of the composite are consistent with the characteristic peaks of TiO_2 and Ti_3C_2. For example, Ti_3C_2 (002), (004), (006), (105) and other characteristic peaks, TiO_2 (101), (004), (200) and other characteristic peaks are reflected in the diffraction peak of the composite material. This indicates that Ti_3C_2/TiO_2 composite is a coexistence structure of TiO_2 and Ti_3C_2[30], and the Ti_3C_2/TiO_2 composite has been successfully prepared.

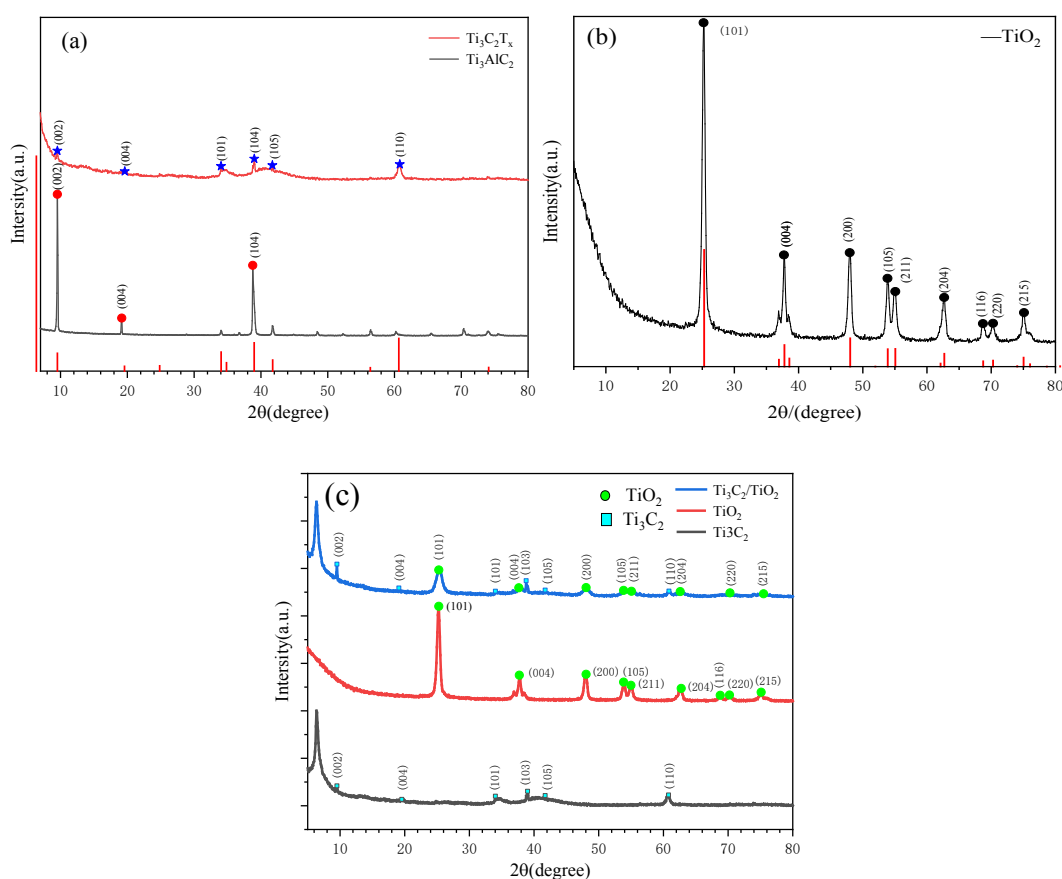Fig. 1. XRD patterns of (a) Ti_3AlC_2 and Ti_3C_2MXene, (b) TiO_2 and (c) Ti_3C_2, TiO_2 and Ti_3C_2/ TiO_2 nanocomposites.

The morphology of $Ti_3C_2T_x$, TiO_2 and $TiO_2/ Ti_3C_2T_x$ were characterized by FESEM. Fig. 2 presents the micromorphology of $Ti_3C_2T_x$ and TiO_2. It can be seen from Fig. 2a that the etched $Ti_3C_2T_x$ MXene has an "accordion" morphology with a multi-layer structure. The spacing between

layers is different, which intuitively reflects the good etching effect and also proves that the preparation of Ti_3C_2 is very successful. The SEM micrograph of TiO_2 is shown in Fig. 2b. As can be seen from the figure, the average size of pure TiO_2 is 1-4 μm and is composed of a large number of irregular small particles.

Fig. 2c and d shows the SEM image of $Ti_3C_2T_x/TiO_2$ composites. It can be seen from Fig. 2c that a large amount of TiO_2 grows on the surface of $Ti_3C_2T_x$. Some TiO_2 even grows between $Ti_3C_2T_x$ layers, as shown in Fig. 2d, achieving fine-tuning of the $Ti_3C_2T_x$ interlayer structure by TiO_2 particles. The existence of these intercalated TiO_2 particles effectively prevents the accumulation of $Ti_3C_2T_x$ sheets. The TiO_2 particle size in the $Ti_3C_2T_x /TiO_2$ composite material is reduced, and the agglomeration phenomenon is also significantly reduced compared with the TiO_2 sample.
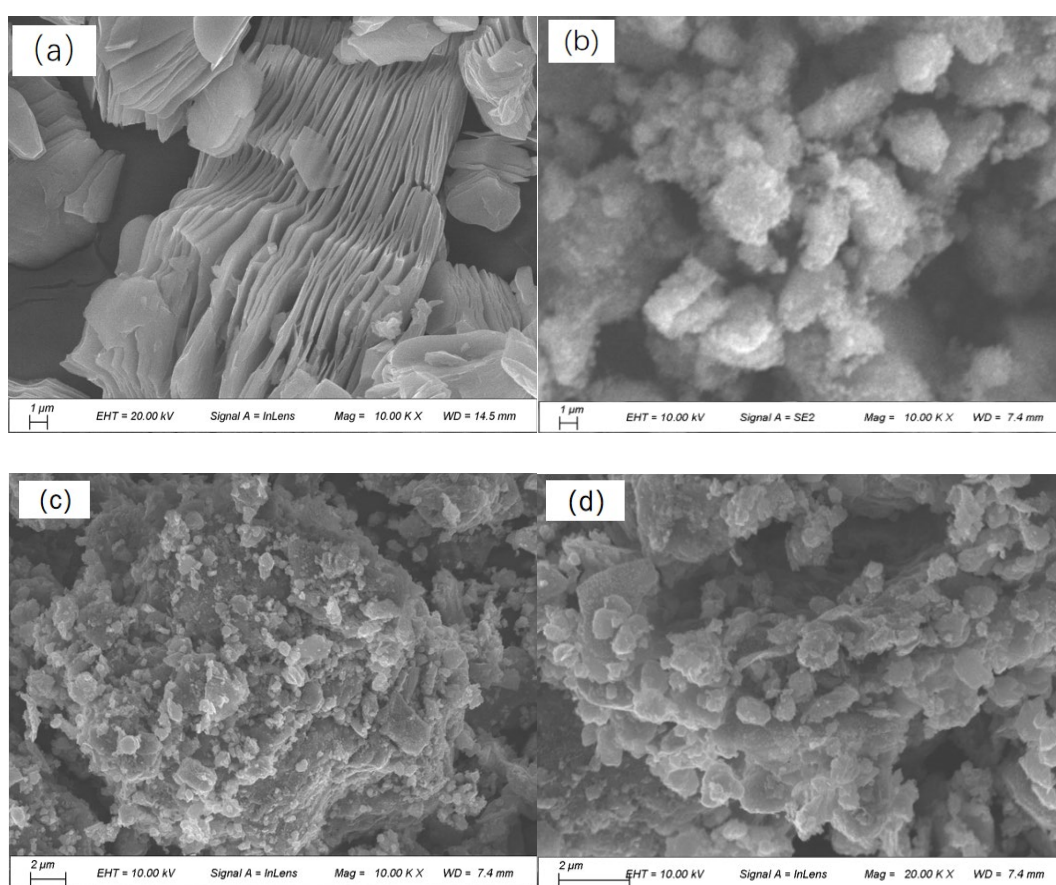

Fig. 2. SEM images of Ti_3C_2 (a), TiO_2 (b) and $Ti_3C_2T_x/TiO_2$ composites (c and d).

3.2. Tribology performance of $Ti_3C_2T_x/TiO_2$ composites

In order to explore the tribological behavior of $Ti_3C_2T_x/TiO_2$ composite materials as lubricating oil additives, three groups of tribological experiments were conducted under different experimental conditions such as different additive concentrations, different working loads, and different working speeds.

3.2.1. Analysis of tribological properties with different additive concentrations

The prepared $Ti_3C_2T_x/TiO_2$ composite material was added to the PAO6 base oil in mass percentages of 0.0wt%, 0.5wt%, 1.0wt%, 1.5wt% and 2.0wt% respectively to prepare the lubricating oil. And the test was conducted for 10 minutes under the experimental conditions of a working load of 15N and a working speed of 120rpm.

The test results are shown in Fig. 3. As can be seen from the Fig. 3a, the friction coefficient of the base oil is about 0.3, and the friction coefficient of the lubricant containing 0.5wt%, 1.0wt% and 1.5wt%$Ti_3C_2T_x/TiO_2$ composite material is 0.25, 0.17 and 0.23, respectively. It can be seen that the introduction of $Ti_3C_2T_x/TiO_2$ composite material can reduce friction. The reason is that the $Ti_3C_2T_x/TiO_2$ composite particles dispersed in the lubricating oil can form a protective film by depositing on the surface after being captured by the friction pair during the friction process, thereby reducing the shear strength between the friction pairs. The damaged surfaces of the friction pair are also filled and repaired, thereby reducing the friction coefficient. But when the $Ti_3C_2T_x/TiO_2$ content in the lubricating oil reaches or exceeds 2.0wt%, the friction coefficient will be higher than the base oil. The reason is that when the concentration is too high, $Ti_3C_2T_x/TiO_2$ is prone to agglomeration, making it difficult to enter the friction contact area, resulting in an increase in the friction coefficient.

Fig. 3b shows the average wear rate of the steel disc after testing with different concentrations of $Ti_3C_2T_x/TiO_2$ lubricants. As can be seen from the figure, the average wear rate of PAO6 base oil is 5.4×10^{-5}mg/s, and the average wear rate of lubricating oil containing 0.5wt%, 1.0wt%, 1.5wt% and 2.0wt% $Ti_3C_2T_x/TiO_2$ is respectively 4.12×10^{-5}, 1.73×10^{-5}, 3.72×10^{-5}mg/s and 5.62×10^{-5}mg/s. Experimental results show that the wear rate of lubricating oil containing 1.0wt% composite material is about 70.0% lower than that of pure base oil, indicating that $Ti_3C_2T_x/TiO_2$ composite material has a good friction reducing effect as an additive. The above experimental results prove that when the $Ti_3C_2T_x/TiO_2$ addition concentration is 1.0 wt%, the friction reducing and wear resistance properties of the lubricating oil are optimal.
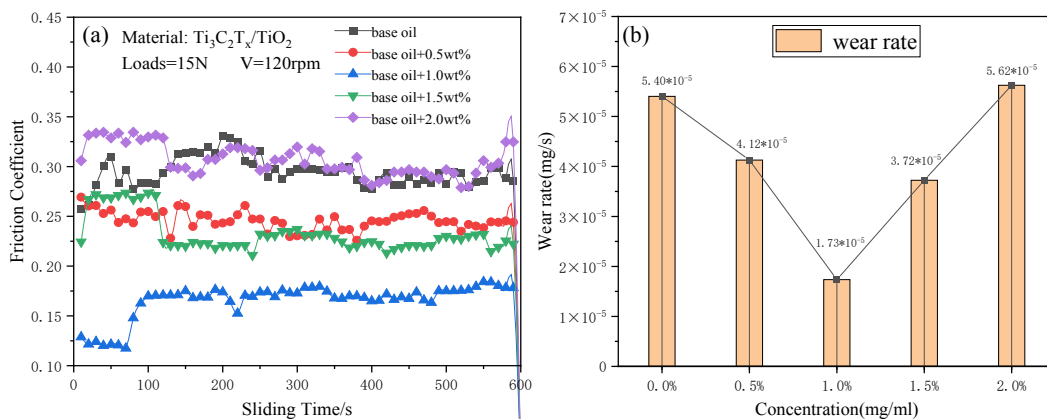

Fig 3. (a) The relationship between friction coefficient and time of lubricants containing different additive concentrations of $Ti_3C_2T_x/TiO_2$ composites. (b) Average wear rate plots of lubricants containing $Ti_3C_2T_x/TiO_2$ composites with different additive concentrations.

At the same time, the wear scars of the surface of the steel disc after the friction test were also analyzed. The SEM images of the surface wear scar are shown in Fig. 4. It can be seen that when the lubricating material is PAO6 base oil, the wear traces show some rough, thick, and deep grooves, and indicating that severe wear occurred on the steel disc surfaces, as shown in Fig. 4a. Compared with the wear scars of the base oil, the wear scars of the base oil containing 0.5wt%, 1.0wt% and 1.5wt% Ti$_3$C$_2$T$_x$/TiO$_2$ composite materials are flat and smooth, as shown in Fig. 4b to 4d. In addition, the steel disc lubricated with 1wt% Ti$_3$C$_2$T$_x$/TiO$_2$ composites has the shallowest wear mark depth, which once again proves that this concentration of lubricant has the best friction reducing effect. However, when the content of composite materials in the lubricating oil exceeds 2.0wt%, many peeling areas appear on the wear surface, and there are some grooves distributed along the sliding direction, indicating increased wear on the steel plate surface. The reason may be that when the concentration of composite materials in the lubricating oil is too high, agglomeration easily occurs, resulting in the inability to form a uniform lubricating film on the surface of the friction pair.
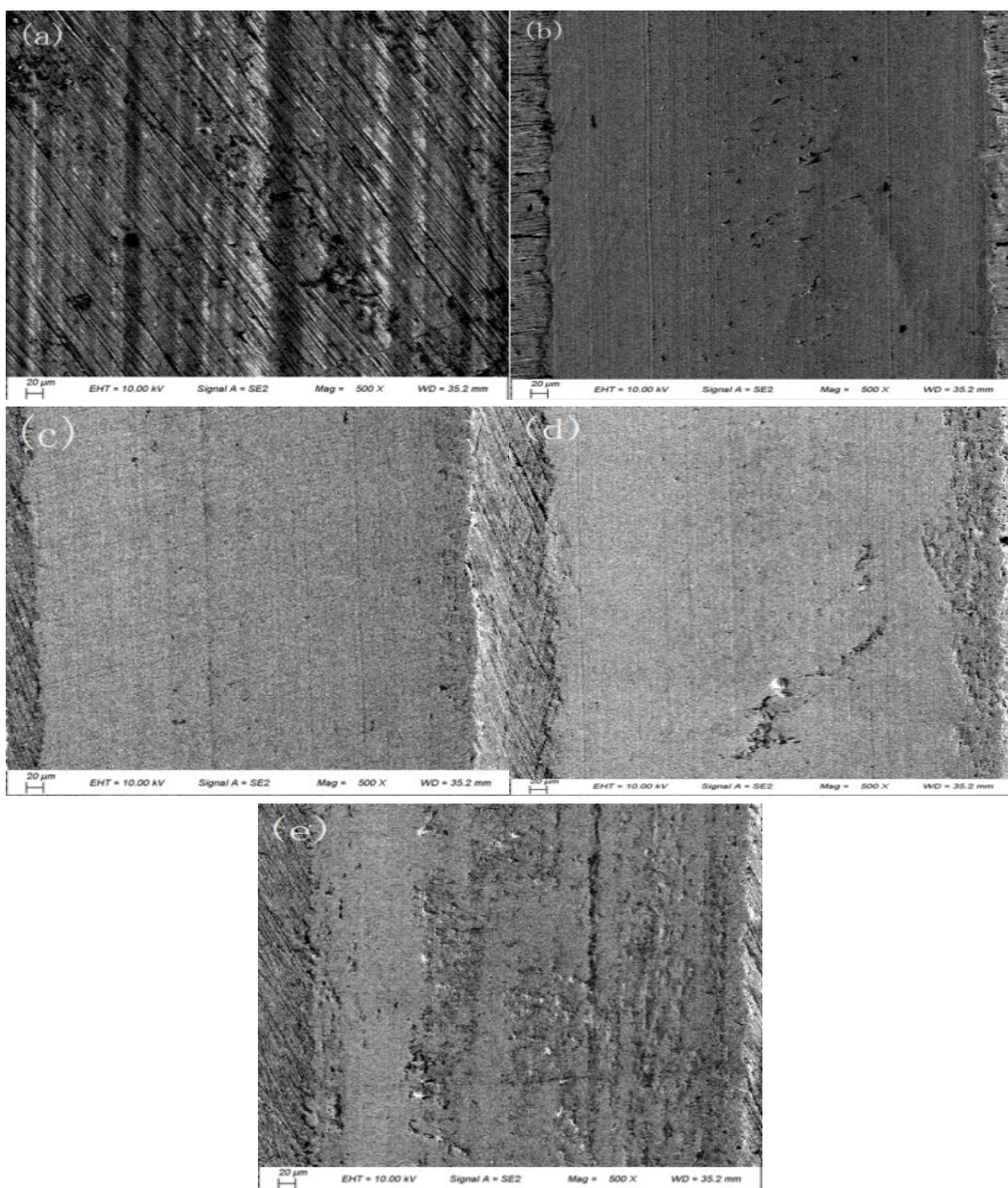

Fig. 4. SEM images of the wear scars lubricated by of PAO6 base oil with different Ti$_3$C$_2$T$_x$/TiO$_2$ composites addition concentrations: 0% (a), 0.5wt% (b), 1.0wt% (c), 1.5wt% (d) and 2wt% (e).

3.2.2. Effect of working load on tribological properties

The prepared $Ti_3C_2T_x/TiO_2$ composite material was added to the PAO6 base oil at a mass percentage of 1.0wt%. Under the test conditions of 120rpm rotation speed, 10mm reciprocating stroke, and 10min working time, the lubricating oil was tested under different loads. The test results are shown in Fig. 5. It can be seen that when the load is 5N, the friction coefficient is the largest, about 0.35. As the load increases, the friction coefficient decreases. When the load reaches 15N, the friction coefficient is the smallest and most stable. The reason is that during the low-load friction process, the $Ti_3C_2T_x/TiO_2$ composite particles in the lubricant are captured by the friction pair and form a precipitation film on the friction surface, which reduces the direct contact of the friction surface, so the friction pair coefficient decreases. When the load reaches 15N, the layered structure of the $Ti_3C_2T_x/TiO_2$ composite material separates and is adsorbed on the friction surface. Moreover, the TiO_2 nanoparticles on the surface of $Ti_3C_2T_x$ are small in size and have good ductility, which can repair the friction surface, thereby further reducing the friction coefficient. However, as the load continues to increase, the friction coefficient will fluctuate irregularly, because when the load reaches a certain value, it is easy to destroy the precipitation film formed on the surface, thereby increasing the friction coefficient and producing larger fluctuations.
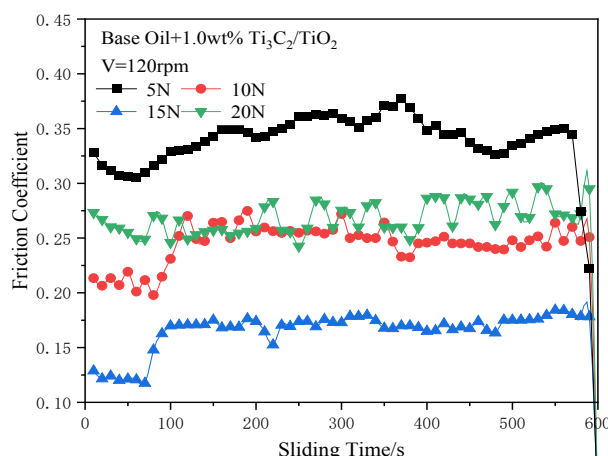

Fig. 5. COF diagram of a lubricant containing 1.0wt%$Ti_3C_2T_x/TiO_2$ composite under different loads.

3.2.3. Effect of working speed on tribological properties

In order to further analyze the tribological properties of $Ti_3C_2T_x/TiO_2$ composite materials, comparative experiments were conducted at different working speeds on lubricating oil with a $Ti_3C_2T_x/TiO_2$ concentration of 1.0wt%. The experimental load was 15N, the working time was 10min, the reciprocating stroke was 10mm, and the working speed was 120rpm, 180rpm, 240rpm and 300rpm, respectively. The experimental test results are shown in Figure 6. It can be seen from the figure that when the rotation speed is 120 rpm, the friction coefficient is the smallest, about 0.17. As the rotational speed continues to increase, the friction coefficient first increases and then decreases. The reason for this change may be that as the sliding speed increases, the thickness of the lubricating film becomes thinner, resulting in adhesive wear caused by direct contact between surface protrusions, thereby increasing the friction coefficient. When the sliding speed increases to a certain value, the convex parts between the surfaces undergo shear plastic deformation, which

promotes the accumulation of dislocations, improves the surface strength through dislocation strengthening, and prevents adhesive wear, thus reducing the friction coefficient.
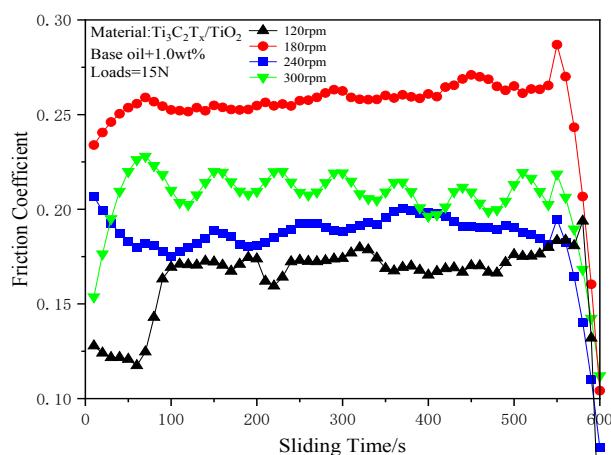

Fig. 6. COF diagram of a lubricant containing 1.0wt%Ti₃C₂Tₓ/TiO₂ composite at different working speeds.

3.3. Lubrication mechanism analysis

In order to reveal the lubrication mechanism of $Ti_3C_2T_x/TiO_2$ composite nanosheets as lubricating oil additive, the wear scars of steel discs were characterized by energy-dispersive X-ray spectroscopy (EDS). The results are shown in Fig. 7. Ti, O and C elements were detected in the wear scars, indicating that the $Ti_3C_2T_x/TiO_2$ composite material entered the friction contact area with the lubricating oil and covered the surface of the friction pair, preventing the friction pair from direct contact.

According to the surface analysis of wear scars, the friction reduction and anti-wear effects of $Ti_3C_2T_x/TiO_2$ composite materials can be summarized into the following aspects. First, the $Ti_3C_2T_x/TiO_2$ composite material is evenly and stably dispersed in the PAO6 base oil, making it easy to enter the contact area and provide continuous lubrication, which is the primary condition for its lubrication ability to be fully exerted[31]. Secondly, the interlayer spacing of MXene nanosheets in the composite material is enlarged due to TiO_2 particles, resulting in further weakening of its shear strength. Relative sliding between layers offsets some of the friction during mechanical movement[32,33]. Third, the $Ti_3C_2T_x/TiO_2$ composite material can be embedded in the grooves on the surface of the friction pair, reducing the probability of direct contact between the bumps on the surface of the friction pair, thereby avoiding serious wear. Specifically, small-sized TiO_2 particles are peeled off from the composite material during the sliding process, playing the dual role of sharing friction and filling grooves. On the other hand, the high temperature generated by friction and sliding promotes the adsorption and deposition of additives on the surface of the friction pair, forming a dense lubricating film on the surface of the friction pair, preventing direct contact between the friction pairs and reducing the wear of the friction pair. In short, the introduction of $Ti_3C_2T_x/TiO_2$ composite material effectively prevents the collision of the friction pair surface, and ultimately achieves effective protection of the friction pair during the sliding process.
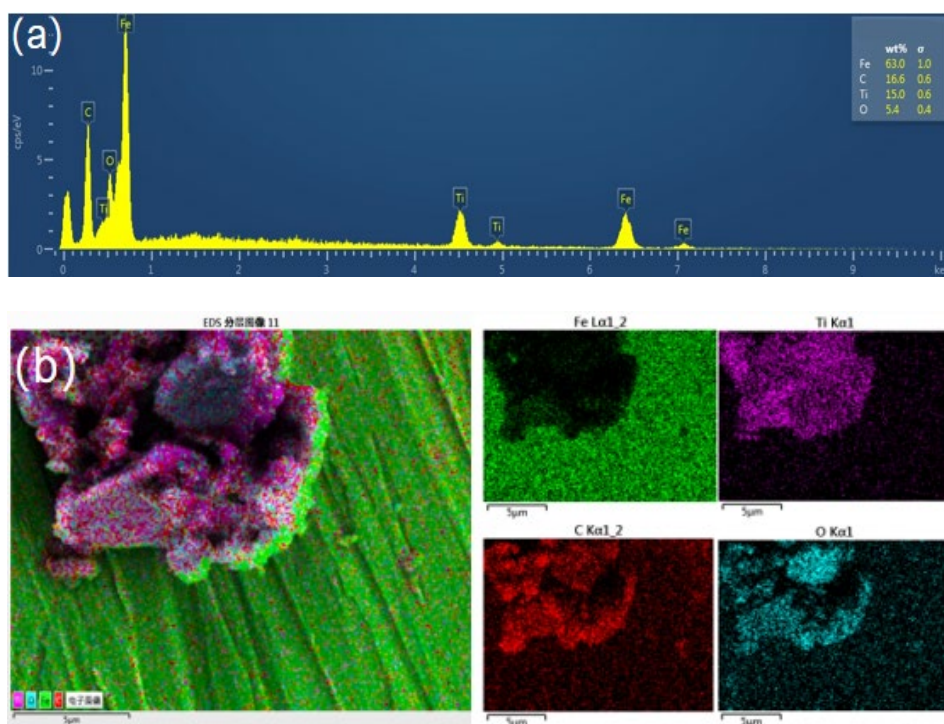
Fig. 7.(a) Energy spectrum content of Ti$_3$C$_2$T$_x$/TiO$_2$ composites. (b) Energy spectrum distribution of Ti$_3$C$_2$T$_x$/TiO$_2$ composites.

4. Conclusion

In summary, Ti$_3$C$_2$T$_x$/TiO$_2$ composite nanomaterials have been successfully fabricated by a simple hydrothermal reaction process, and TiO$_2$ particles were evenly distributed on the intercalation and surface of Ti$_3$C$_2$T$_x$ nanosheets. PAO6 base oil added with Ti$_3$C$_2$T$_x$/TiO$_2$ composite materials showed good friction and wear properties. The tribological experiments indicated that the lubricating performance was able to be improved by the introduction of Ti$_3$C$_2$T$_x$/TiO$_2$ composite materials as additives to base oil. And the friction coefficient and wear rate are related to the concentration of additives in the base oil. When the additive concentration is 1.0wt%, the friction reducing effect of the lubricating oil is the best, and the wear rate is about 70.0% lower than that of the pure base oil. In addition, working load and working speed also affect the tribological properties of lubricants. By analyzing the wear traces on the surface of the steel plate, it can be determined that the friction reduction mechanism of Ti$_3$C$_2$T$_x$/TiO$_2$ material is that nanomaterials enter the two rubbing surfaces and form a thin physical tribofilm on the rubing surface. This tribofilm can not only bear the load of the steel ball but also prevent them from direct contact. The excellent tribological properties indicate that the as-prepared Ti$_3$C$_2$T$_x$/TiO$_2$ composite materials will be useful for its further industrial application as a good oil additive in the future.

Acknowledgements

References

[1] J. Luo, M. Liu, L. Ma, Nano Energy, 86,106092(2021);
https://doi.org/10.1016/j.nanoen.2021.106092
[2] Y. Meng, J. Xu, Z. Jin, et al., Friction, 8, 221-300(2020);
https://doi.org/10.1007/s40544-020-0367-2
[3] E. Garbar, I. I. Sher, R. Shneck, Industrial lubrication and Tribology,52(4), 186-192(2000);
https://doi.org/10.1108/00368790010333638
[4] Q. Chen, S. Zheng, S. Yang, et al., Journal of sol-gel science and technology, 61,
501-508(2012); https://doi.org/10.1007/s10971-011-2651-0
[5] J. Wang, Y. Zhou, Annual Review of Materials Research, 39, 415-443(2009);
https://doi.org/10.1146/annurev-matsci-082908-145340
[6] X. F. Zhang, Y. Guo, Y. J. Li, et al., Chinese Chemical Letters,30(2), 502-504(2019);
https://doi.org/10.1016/j.cclet.2018.07.007
[7] Y. Wei, P. Zhang, R. A. Soomro, et al., Advanced materials, 33(39),2103148(2021);
https://doi.org/10.1002/adma.202103148
[8] Z. Cheng, Z. Du, H. Chen, et al., Advanced Materials,2302141(2023);
https://doi.org/10.1002/adma.202302141
[9] S. Venkateshalu, J. Cherusseri, M. Karnan, et al., ACS omega, 5(29), 17983-17992(2020);
https://doi.org/10.1016/j.jssc.2019.120947
[10] M. Naguib, J. Halim, J. Lu, et al., Journal of the American Chemical Society, 135(43),
15966-15969(2013); https://doi.org/10.1021/ja405735d
[11] S. Wang, J. X. Li, Y. L. Du, et al., Computational Materials Science, 83, 290-293(2014);
https://doi.org/10.1016/j.commatsci.2013.11.025
[12] M. Sygnatowicz, R. A. Cutler, D. K. Shetty, Journal of the American Ceramic Society,
98(8),2601-2608(2015); https://doi.org/10.1111/jace.13635
[13] M. Naguib, J. Come, B. Dyatkin, et al., Electrochemistry Communications,16(1),
61-64(2012); https://doi.org/10.1016/j.elecom.2012.01.002
[14] P. Zhang, Q. Zhu, R. A. Soomro, et al., Advanced Functional Materials,
30(47),2000922(2020); https://doi.org/10.1002/adfm.202000922
[15] Y. Liu, X.F. Zhang, S.L. Dong, et al, Journal of Materials Science, 52, 2200-2209 (2017);
https://doi.org/10.1007/s10853-016-0509-0
[16] Y. Wang, Y. He, Q. Lai, et al, Journal of environmental sciences, 26(11),2139-2177(2014);
https://doi.org/10.1016/j.jes.2014.09.023
[17] J. He, J. Cheng , I. M. C. Lo, Water Research, 190,116705(2021);
https://doi.org/10.1016/j.watres.2020.116705
[18] C. X. Shan, X. Hou, K. L. Choy, Surface and Coatings Technology, 202(11),2399-2402(2008);
https://doi.org/10.1016/j.surfcoat.2007.08.066
[19] Y. Hu, S. Huang, S. Liu, et al., Applied surface science,258(19),7460-7464(2012);
https://doi.org/10.1016/j.apsusc.2012.04.061
[20] C. C. Trapalis, P. Keivanidis, G. Kordas, et al., Thin Solid Films,433(1-2),186-190(2003);
https://doi.org/10.1016/S0040-6090(03)00331-6
[21] S.S. Mirjavadi, M. Alipour, S. Emamian, S. Kord, A.M.S. Hamouda, P.G. Koppad, et al.,
Journal of Alloys Compounds, 712, 795–803 (2017); https://doi.org/10.1016/j.jallcom.2017.04.114
[22] H.J. Song, Z.Z. Zhang, Tribology International, 41, 396–403(2008);
https://doi.org/10.1016/j.triboint.2007.09.004

[23] Q. Xue, W. Liu, Z. Zhang, Wear, 213(1-2),29-32(1997); https://doi.org/10.1016/S0043-1648(97)00200-7

[24] A. Krishnamurthy, K. A. Razak, B. S. Halemani, et al., Materials Today: Proceedings, 47,6180-6184(2021); https://doi.org/10.1016/j.matpr.2021.05.083

[25] W. Li, S. Zheng, B. Cao, S. Ma, et al., Journal of Nanoparticle Research, 13, 2129–2137(2011); https://doi.org/10.1007/s11051-010-9970-x

[26] I. Piwonski, K. Soliwoda, Ceramics International, 36(1), 47–54(2010); https://doi.org/10.1016/j.ceramint.2009.06.024

[27] M. Avella, M.E. Errico, E. Martuscelli, Nano Letters, 1(4), 213–217(2001); https://doi.org/10.1021/nl015518v

[28] S. Venkateshalu, J. Cherusseri, M. Karnan, et al., ACS Omega, 5(29), 17983-17992(2020); https://doi.org/10.1021/acsomega.0c01215

[29] B. Anasori, M. R. Lukatskaya, Y. Gogotsi, Nature Reviews Materials, 2(2), 1-17(2017); https://doi.org/10.1038/natrevmats.2016.98

[30] J. X. Yang, W. B. Yu, C. F. Li, et al., Chemical Engineering Journal, 420,129695(2021); https://doi.org/10.1016/j.cej.2021.129695

[31] J. Guo, P. Wu, C. Zeng, et al., Tribology International, 170, 107500(2022); https://doi.org/10.1016/j.triboint.2022.107500

[32] S. Luo, S. Patole, S. Anwer, et al., Nanotechnology,31(39),395704(2020); https://iopscience.iop.org/article/10.1088/1361-6528/ab94dd

[33] H. Li, Z. P. Hou, X. H. Zhang, Digest Journal of Nanomaterials and Biostructures, 18(4), 1395-1407; https://doi.org/10.15251/DJNB.2023.184.1395